Applied Environmental Research
- RESEARCH FOR SUSTAINABLE PLANET -

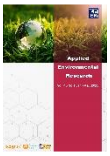

Research Article

Development of Highly Effective Sulfonic Acid–Functionalized NR/MS Nanocomposites for Biodiesel Production

Sakdinun Nuntang[1,*], Satit Yousatit[2], Toshiyuki Yokoi[3], Chawalit Ngamcharussrivichai[2,4,5]

[1] Industrial Chemistry Innovation Program, Faculty of Science, Maejo University, Chiang Mai 50290, Thailand
[2] Department of Chemical Technology, Faculty of Science, Chulalongkorn University, Pathumwan, Bangkok 10330, Thailand
[3] Chemical Resources Laboratory, Tokyo Institute of Technology, 4259 Nagatsuta, Midori-ku, Yokohama 226-8503, Japan
[4] Center of Excellence on Petrochemical and Materials Technology (PETROMAT), Chulalongkorn University, Pathumwan, Bangkok 10330, Thailand
[5] Center of Excellence in Catalysis for Bioenergy and Renewable Chemicals (CBRC), Faculty of Science, Chulalongkorn University, Pathumwan, Bangkok 10330, Thailand

*Corresponding Email: Sakdinun.nt@gmail.com

Abstract

The acidic natural rubber/wormhole-like mesostructured silica nanocomposites (NR/WMS–SO_3H) were successfully functionalized with propylsulfonic acid and arenesulfonic acid via a cocondensation method using 3-mercaptopropyl trimethoxysilane (MPTMS) and 2-(4-chloro-sulfonylphenyl) ethyltrimethoxy silane (CSPTMS), respectively. Compared with organosulfonic acid-functionalized wormhole-like mesostructured silica (WMS–SO_3H), NR/WMS–SO_3H demonstrated increased hydrophobicity while maintaining mesoporosity and a large surface area. The catalytic performance of the synthesized solid acids was subsequently evaluated via batch esterification of palmitic acid with methanol to generate fatty acid methyl esters for biodiesel synthesis. Compared with WMS–SO3H, NR/WMS–SO_3H demonstrated superior catalytic activity, which was attributed to the synergistic interaction between the strongly acidic functional groups and surface hydropho-bicity. The NR/WMS-SO_3H catalysts demonstrated novel properties with a large surface area and high acidity and prevented hydrolysis, paving the way for further study to produce other high-value ester products via esterification since they exhibited high conversion of free fatty acids.

ARTICLE HISTORY

Received: 3 Dec. 2024
Accepted: 12 Jun. 2025
Published: 17 Jun. 2025

KEYWORDS

Nanocomposite;
Natural rubber;
Wormhole-like mesostructured silica;
Sulfonic acid;
Biodiesel

Introduction

Biodiesel is an alternative to standard diesel fuel that may be made from vegetable oils or animal fats. It is renewable and biodegradable, resulting in less air pollution than petroleum-based diesel and reducing our reliance on fossil fuels [1]. The production of biodiesel can be achieved through esterification, a process in which carboxylic molecules found in vegetable oils or animal fats undergo a chemical reaction with short-chain alcohols, such as methanol or ethanol, facilitated by an acid catalyst [2–3]. The recent application of solid acid catalysts for this reaction has received attention because of their high selectivity, ease of separation, ease of recovery and reduced amount of waste. Many reports have prepared solid acid catalysts by functionalizing sulfonic groups onto a mesoporous silica framework. A catalytic activity and selectivity enhancement during the esterification process has been reported [4–5].

The exploration of wormhole-like mesostructured silica functionalized with organosulfonic acid groups presents attractive opportunities for catalysis in esterification. Their unique wormhole-like porous structure, combined with a high surface area and strong sulfonic acid groups, enhances their catalytic potential. Nonetheless, the remaining silanol groups on the surface of the produced materials increased the hydrophilicity and hindered the reaction due to the readsorption of H_2O at the acid sites [6–7]. Recently, natural rubber/wormhole-like mesostructured silica nanocomposites functionalized with organosulfonic acid groups have received increasing interest for application as catalysts for esterification reactions. This material possesses large pore volumes, a high specific surface area, a narrow pore size distribution, high acidity and hydrophobicity. Moreover, its hydrophobic property can reduce the hydrolysis of ester to substances because H2O cannot be reabsorbed at its acid sites [8–

10]. The functionalization of mesoporous silica with sulfonic acid leads to efficient solid acids, which exhibit improved catalytic properties attributed to increased amounts and strengths of Brønsted acid sites. Organofunctional groups, including propyl sulfonic (–$PrSO_3H$) and arene sulfonic acid (–$ArSO_3H$), can be attached to the mesoporous silica surface through postgrafting or direct cocondensation [11–12]. The materials that have been functionalized through postgrafting demonstrate a generally organized mesostructure; however, there is a nonuniform distribution of organic moieties. This is attributed to the aggregation of organosilane precursors at the pore mouths of the mesoporous channels and on the external surfaces of the mesoporous materials [13]. The cocondensation represents an individual process where the hydrolysis and condensation of tetraethoxysilane and organosilane precursors take place concurrently around the micellar surfactant template. Therefore, organosilanes are well distributed on the mesoporous silica surface. [14]. However, in the past, few comparative studies have been conducted on the effectiveness of propyl sulfonic and arene sulfonic acids functionalized on the surface of mesoporous silica composite materials in esterification to maximize the yield of ester products. have shown successful results for acid-catalyzed reactions [11,15].

The current study aims to utilize organosulfonic acid groups (–$PrSO_3H$ and –$ArSO_3H$) through a cocondensation process, with the advantages of a natural rubber/wormhole-like mesostructured silica nanocomposite, to create nanocomposite catalysts characterized by high acidity and hydrophobicity. This investigation focuses on the effects of surface modification via various organosulfonic acid groups on the physicochemical properties of the resulting NR/WMS–SO3H materials in comparison with those of sulfonic acid-functionalized wormhole-like mesostructured silica (WMS–SO_3H). The NR/WMS–SO_3H catalysts will be examined for their ability to produce fatty acid methyl esters (FAME) for biodiesel production.

Materials and methods

1) Materials and chemical reagents

Tetraethyl orthosilicate (TEOS; analytical grade 99%), 3-mercaptopropyltrimethoxysilane (MPTMS; analytical grade 99%), 2-(4-chloro-sulfonyl phenyl) ethyl trimethoxysilane (CSPTMS; analytical grade 98%), hydrogen peroxide solution (H_2O_2; analytical grade), and tetradecylamine (TDA; analytical grade 95%) were acquired from Sigma–Aldrich (USA). Tetrahydrofuran (THF; analytical grade 99.5%) was sourced from QREC Chemicals Co. Ltd. (New Zealand). Palmitic acid ($CH_3(CH_2)$14COOH; analytical grade > 99%), sulfuric acid (H_2SO_4; analytical grade 98%), and absolute methanol and ethanol (analytical grade 99.5%) were acquired from Merck Millipore Ltd. (Germany). The NR (standard Thai rubber, grade 5 L) was supplied by Thai Hua Chumporn Natural Rubber Co. Ltd. in Thailand. All materials and reagents were utilized as received without additional purification.

2) Preparation of sulfonic acid-functionalized mesoporous silica

2.1) Synthesis of NR/WMS–$PrSO_3H$ and WMS–$PrSO_3H$

The NR/WMS–$PrSO_3H$ nanocomposite was prepared according to previous methods [8–10]. Initially, 0.5 g of each NR sample was immersed in TEOS at room temperature for 16 hours. The swollen NR sheet was subsequently dissolved in THF to yield a colloidal mixture. TDA was then combined with the mixture, and TEOS was added dropwise while stirring. After one hour, deionized water, MPTMS, and H_2O_2 were added sequentially to the mixture while stirring, and the mixture was subsequently allowed to stand at 40 °C for 1 hour. The molar composition of the synthesis mixture was as follows: 0.10 TEOS, 0.04 TDA, 5.89 H_2O, 0.37 THF, 0.01 NR, 0.02 MPTMS, and 0.14 H_2O_2. The gel was aged at 40 °C for 3 days, after which it was precipitated in 100 mL of ethanol. The solid product was obtained through filtration and subsequently dried at 110 °C for 2 hours. Finally, the amine template was extracted from the synthesized nanocomposite by treatment with a 0.05 M H_2SO_4/ethanol solution at 70 °C for 4 hours. WMS–$PrSO_3H$ was synthesized via the same procedure, excluding the addition of the NR sheet.

2.2) Synthesis of NR/WMS–$ArSO_3H$ and WMS–$ArSO_3H$

The NR/WMS–ArSO3H nanocomposite was prepared by adapting it from previous reports [8–10] and Mbaraka et al. [15]. Initially, 1 g of NR sheet was immersed in TEOS at room temperature and subsequently dissolved in THF, following the same procedure as the preparation of NR/WMS-$PrSO_3H$. TDA was subsequently combined with the NR mixture, and TEOS was added dropwise while stirring. After 1 hour, deionized water and CSPTMS were introduced dropwise. The mixture was stirred for 20 hours at 35 °C, followed by aging at 95 °C for an additional 24 hours. The molar composition of the synthesis mixture was 0.10 TEOS, 0.04 TDA, 5.89 H_2O, 0.37 THF, 0.01 NR, and 0.02 CPTMS. A white gel formed and subsequently precipitated in 100 mL of ethanol. Finally, the retrieval of the solid result and the process of removing the template followed the same steps as the preparation of NR/WMS–$PrSO_3H$. In addition, WMS−$ArSO_3H$ was synthesized via the same procedure, excluding the addition of the NR sheet.

2.3) Characterization of sulfonic acid-functionalized mesoporous silica

X-ray diffraction patterns were acquired via a Rigaku SmartLab diffractometer employing Cu Kα radiation (λ = 0.154 nm). The X-ray source functioned at 40 kV and 40 mA, with counts collected every 0.02° (2θ) at a scanning rate of 1° (2θ)/min.

The characterization of the functional groups in these materials was conducted via a Perkin-Elmer Spectrum One Fourier transform infrared spectrometer (FTIR). The sample wafer was prepared via the KBr method. The FTIR spectra were acquired in transmittance mode across the range of 400-4,000 cm^{-1}.

N$_2$ adsorption–desorption was measured at -196 °C via a BEL Japan BELSORP-mini II instrument to determine the textural properties of the materials. The sample weight, initially approximately 40 mg, was precisely measured following pretreatment at 150 °C for 2 hours.

The morphology of the sample was assessed by scanning electron microscopy (SEM). SEM images were captured via a TESCAN VEGA3 scanning electron microscope operating at 30 kV. The samples on the carbon tape were examined with a gold coating applied.

The acid content of the functionalized materials was assessed through acid–base titration. In general, 0.5 g of the sample was equilibrated with a 20-mL solution of THF and ethanol (50% (v/v)) and stirred at room temperature for 18 hours. The resulting mixture was subsequently titrated using a 0.02 M NaOH aqueous solution. Furthermore, a Vario Micro Cube CHNS elemental analyzer from Elementar (UK) was employed to measure the sulfur content in the functionalized materials.

2.4) Esterification of palmitic acid with methanol

The synthesized catalysts were assessed for their catalytic properties in the esterification of palmitic acid (PA) with methanol. The reaction was conducted in a 50-mL closed reactor. In a standard procedure, 3 g of palmitic acid and 7.37 g of methanol (maintaining a 1:20 molar ratio of palmitic acid to methanol) were combined in the reactor. The reaction temperature was maintained at 120 °C via a silicone oil bath. Next, the appropriate catalyst was introduced into the reaction mixture at a concentration of 3 wt.%. A specific volume of the reaction mixture was collected at the 30-minute and 3-hour mark during the reaction to analyze the amount of free fatty acid for calculating the initial rate and conversion, respectively; the mixture was promptly diluted with 1,4-dioxane and subsequently prepared for composition analysis via gas chromatography (Shimadzu, Japan). The palmitic acid conversion and initial rate were determined according to Eqs. 1−2.

$$\text{Palmicitc acid conversion (mol\%)} = \frac{n_{\text{PA, initial}} - n_{\text{PA, remaining}}}{n_{\text{PA, initial}}} \times 100 \qquad \text{(Eq.1)}$$

$$\text{Initial rate (mmol min}^{-1}\text{)} = \frac{n_{\text{PA, used at 30 min}}}{\text{initial time (30 min)}} \times 100 \qquad \text{(Eq.2)}$$

Results and discussion

1) Catalyst characterization

The low-angle powder XRD patterns for the initial WMS, NR/WMS, and modified WMS, NR/WMS materials with –PrSO$_3$H and –ArSO$_3$H groups produced via the cocondensation method are presented in Figure 1. The XRD analysis of these materials facilitated the identification of the ordered arrangement within the mesostructured silica framework. Each of the samples exhibited a distinct broad reflection at a 2θ value between 3.0–6.0°, corresponding to the d100 interplanar spacing [16]. Compared with those of the WMS series, the reflection characteristics of the NR/WMS series shifted toward lower angles, indicating an increase in the size of the unit cell due to the presence of NRs in the silicate framework [16]. The influence of organosulfonic acid group type on the mesostructure was comparable for both functionalized WMS and NR/WMS. Compared with the initial WMS and NR/WMS, the organosulfonic acid functionalized onto WMS and NR/WMS resulted in a lower XRD diffraction peak, resulting in a less ordered mesostructure arrangement. However, the loss of structural ordering was more pronounced in NR/WMS−SO$_3$H than in WMS−SO$_3$H. This finding shows that adding organofunctional groups to NR/WMS had a much greater effect on the structure of the mesostructure than adding functional groups to pure silica WMS.

The functionalization of WMS−SO$_3$H and NR/WMS −SO$_3$H with various organosulfonic acid groups was validated via FTIR spectroscopy, confirming the presence of NR and/or organosulfonic acid groups within the mesostructure, as illustrated in Figure 2. The stretching vibration of the siliceous framework (Si–O–Si) in all the mesoporous samples was observed within the range of 1,000-1,300 cm^{-1}. Furthermore, these materials displayed a broad band at approximately 3,450 cm^{-1}, which can be attributed to surface silanol groups. The pure silica WMS did not present bands related to organic species in its structure (Figure 2A). After functionalization (WMS−SO$_3$H), the bands associated with the −PrSO$_3$H and −ArSO$_3$H groups were identified at 1,340 cm^{-1} (stretching vibration of –SO$_3$ species), 1,360 cm^{-1} (S=O stretching of sulfonic acid groups), and 2850 and 2920 cm^{-1} (C-H stretching of methylene groups) [16]. The results indicated that the mesoporous silica surface was modified through the incorporation of organosulfonic groups. Conversely, NR/WMS exhibited unique bands that aligned with the NR structure at 3,010, 2,920, 2,850, 1,655, and 1,440 cm^{-1} [8], as illustrated in Figure 2B. The functionalization of −PrSO$_3$H and −ArSO$_3$H on the NR/WMS surface was confirmed by the bands at 1340 and 1,360 cm^{-1}, along with a further decrease in the number of surface silanol groups at 3,450 cm^{-1}.

The acidity and sulfur content of the WMS and NR/WMS functionalized with −PrSO$_3$H and −ArSO$_3$H groups, as determined through acid–base titration and CHNS elemental analysis, are presented in Table 1. Both WMS and NR/WMS functionalized with −ArSO$_3$H presented higher sulfur contents than WMS−PrSO$_3$H and NR/WMS −PrSO$_3$H did, and the acidity of these materials increased. These results corresponded with research conducted by Hamoudi et al., who reported the synthesis of propyl- and arene-sulfonic acid group-functionalized periodic mesoporous organosilica via the cocondensation method [17]. This result suggested that the long-chain primary amine template (TDA) in the synthesis mixture could induce the $-\mathrm{ArSO_3H}$ group to condense on the silica surface more easily than the $-\mathrm{PrSO_3H}$ group because of greater hydrophobic interactions. Nevertheless, the acidity of these acidic materials was lower than that of the associated sulfur amount. The results showed that the oxidation process using $\mathrm{H_2O_2}$ could not completely convert all $-\mathrm{SH}$ species into their corresponding $-\mathrm{SO_3H}$ species [10−11]. In addition, the acidity/sulfur content ratio of the NR/WMS−$\mathrm{SO_3H}$ composites was lower than that of the WMS−$\mathrm{SO_3H}$ materials. The reduced ratio observed for the NR/WMS−$\mathrm{SO_3H}$ composites indicated that certain organosulfonic acid groups were integrated into the NR layer, probably due to hydrophobic interactions, as supported by prior research [8].

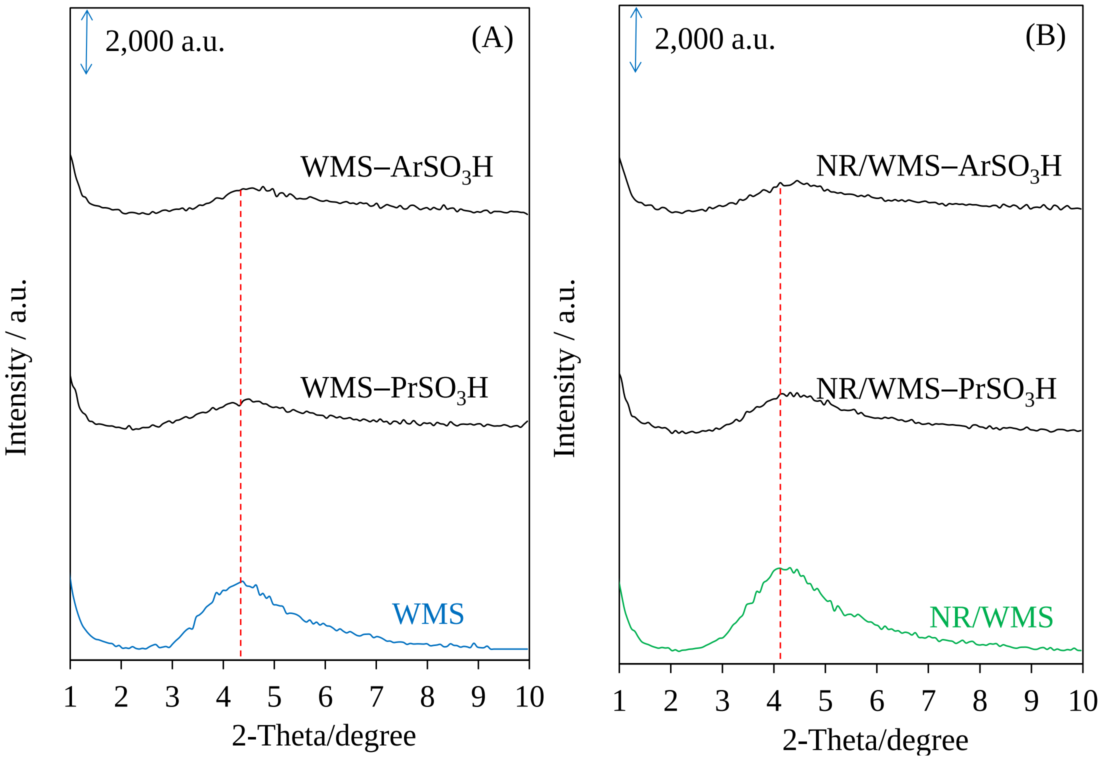

Figure 1 XRD patterns of (A) WMS, WMS–$\mathrm{SO_3H}$ and (B) NR/WMS, NR/WMS–$\mathrm{SO_3H}$ composites.

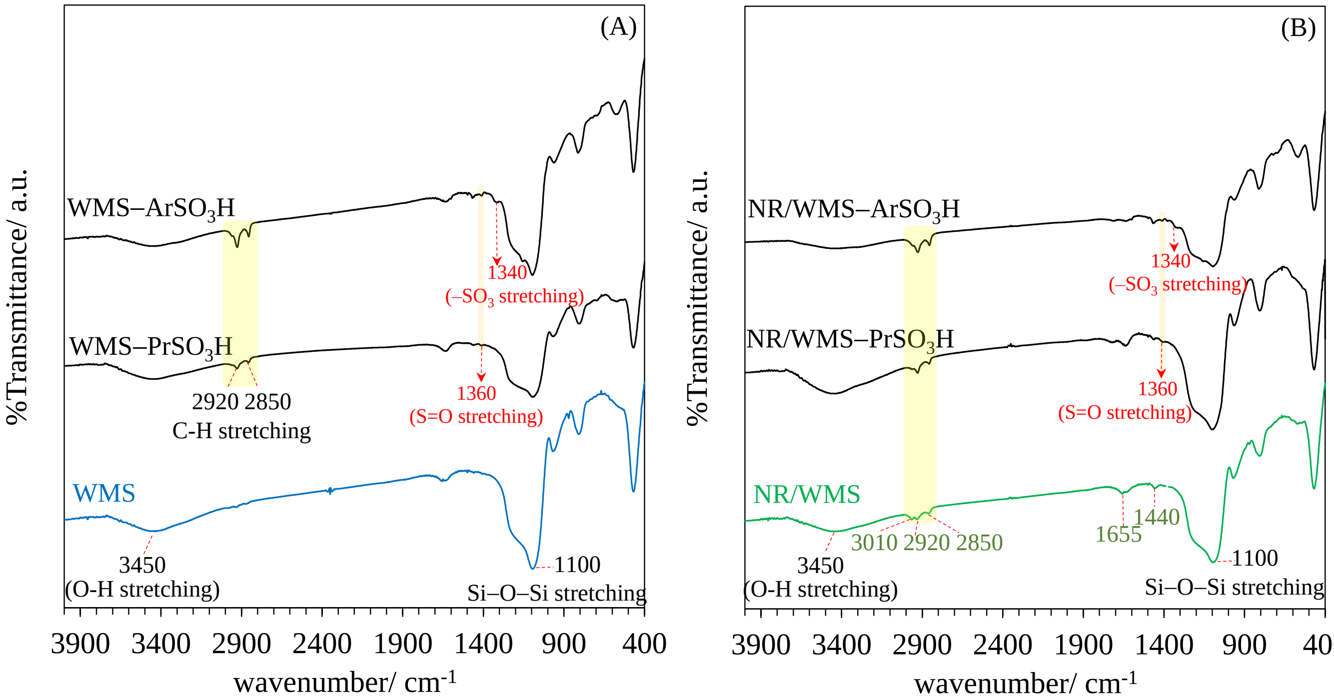

Figure 2 FTIR spectra of (A) WMS, WMS–$\mathrm{SO_3H}$ and (B) NR/WMS, NR/WMS–$\mathrm{SO_3H}$ composites.

The textural properties of the WMS−SO$_3$H and NR/WMS−SO3H materials are summarized in Table 1, together with the initial WMS and NR/WMS data. The N$_2$ adsorption–desorption isotherms and BJH pore size distributions are presented in Figure 3. All the materials exhibited type IV sorption isotherms, as classified by IUPAC. These isotherms showed a hysteresis loop in the P/P_0 range of 0.4–0.7, an identifying characteristic of framework-restricted mesoporous materials. The large hysteresis loop observed at elevated relative pressure (P/P_0 > 0.8) for these materials can be ascribed to the condensation of N$_2$ within the interparticle voids produced by their particle agglomerates. Compared with those of the initial WMS and NR/WMS−SO$_3$H materials, the isotherms of the WMS−SO$_3$H and NR/WMS−SO$_3$H materials presented a reduced N$_2$ adsorbed volume and a smaller hysteresis loop at P/P_0 values of 0.4–0.7. A wider pore size distribution and reduced pore diameter have been observed for WMS−SO$_3$H and NR/WMS−SO$_3$H materials than for primary WMS and NR/WMS materials (Figure 3). The BET surface area (SBET), pore diameter (Dp) and total pore volume (Vt) clearly decreased with increasing organosilane loading (Table 1). These results supported the fact that the −PrSO$_3$H and −ArSO$_3$H groups were functionalized onto the wall of the primary mesoporous silica. The BET surface area (SBET), pore diameter (Dp), and total pore volume (Vt) clearly decreased with increasing organosilane loading (Table 1). These findings confirmed that the −PrSO$_3$H and −ArSO$_3$H groups were successfully functionalized onto the surface of the primary mesoporous silica. In addition, WMS and NR/WMS functionalized with the −ArSO$_3$H group presented lower mesopores than did the mesoporous silica functionalized with the −PrSO$_3$H group. These results are related to the increased acidity and sulfur content of the WMS−ArSO$_3$H and NR/WMS−ArSO$_3$H composites (Table 1).

The SEM images in Figure 4 show the morphologies of the NR/WMS−PrSO$_3$H and NR/WMS−ArSO$_3$H nanocomposites. The inclusion of NR and organosulfonic acid groups within the mesoporous silica framework demonstrated the agglomeration of mesoporous silica particles. Moreover, the NR/WMS−ArSO$_3$H nanocomposite (Figure 4B) revealed a larger aggregate of nanosized silica particles than the NR/WMS−PrSO$_3$H nanocomposite did (Figure 4A). This result corresponded to the lower mesoporosity of NR/WMS−ArSO$_3$H than that of −PrSO$_3$H -functionalized NR/WMS (Table 1).

2) Catalytic study of the esterification of palmitic acid with methanol

The esterification of palmitic acid with methanol was comparatively tested using WMS–SO$_3$H and NR/WMS –SO$_3$H materials, as illustrated in Figure 5. Compared with those of the WMS–SO$_3$H catalysts, the initial rates of the NR/WMS–SO$_3$H composites were lower because of the steric effect resulting from the incorporation of natural rubber in the silica pores. The decrease in the pore size of the NR/WMS–SO$_3$H composites was confirmed by N$_2$ adsorption–desorption measurements, which limit the access of palmitic acid to the active catalytic sites within the pores. This created steric hindrance that slowed molecular diffusion and reduced the number of effective collisions, leading to a lower initial reaction rate, which corresponds with the research conducted by Rác *et al*. [18]. In addition, WMS and NR/WMS functionalized with the –ArSO$_3$H group also presented higher initial rates than did the –PrSO$_3$H-functionalized mesoporous silicas. These results corresponded to the acidity of these materials, as shown in Table 1. In contrast, the NR/WMS–SO$_3$H composites with hydrophobic species confirmed by the FTIR technique (Figure 2) demonstrated greater conversion of palmitic acid than did the WMS–SO$_3$H catalysts. The higher hydrophobicity of the NR/WMS–SO$_3$H catalysts resulted in a deceleration of sulfonic acid–site poisoning and a reduction in the shift of the reaction equilibrium toward hydrolysis. This is attributed to NR's ability to prevent the readsorption of H$_2$O onto sulfonic acid groups, which aligns with findings from prior studies [9−10]. Moreover, NR/WMS–ArSO$_3$H with high acid strength presented the highest conversion of palmitic acid (89.3%) at 3 hours.

Table 1 Physicochemical properties of the WMS, WMS–SO$_3$H, NR/WMS and NR/WMS–SO$_3$H composites

Sample[a]	S_{BET}[b] (m^2 g^{-1})	D_p[c] (*nm*)	V_t[d] (cm^3 g^{-1})	**Acidity**[e] (mmol H$^+$ g^{-1})	**S content**[f] (wt.%)	**Acidity/S content ratio**
WMS	529.7	4.66	1.28	n.d.	n.d.	n.d.
WMS−PrSO$_3$H	534.2	2.71	0.85	1.35	2.38	0.57
WMS−ArSO$_3$H	179.3	2.65	0.55	1.78	3.62	0.49
NR/WMS	465.8	4.22	1.69	n.d.	n.d.	n.d.
NR/WMS−PrSO$_3$H	374.1	2.53	1.34	1.18	2.54	0.46
NR/WMS−ArSO$_3$H	222.6	2.46	1.20	1.61	4.42	0.36

Remark: [a] BET surface area.
[b] Pore diameter, evaluated via the BJH method.
[c] Total pore volume, evaluated by the volume adsorbed at P/P_0 = 0.99.
[d] Determined from acid–base titration.
[e] Determined by a CHNS analyzer.

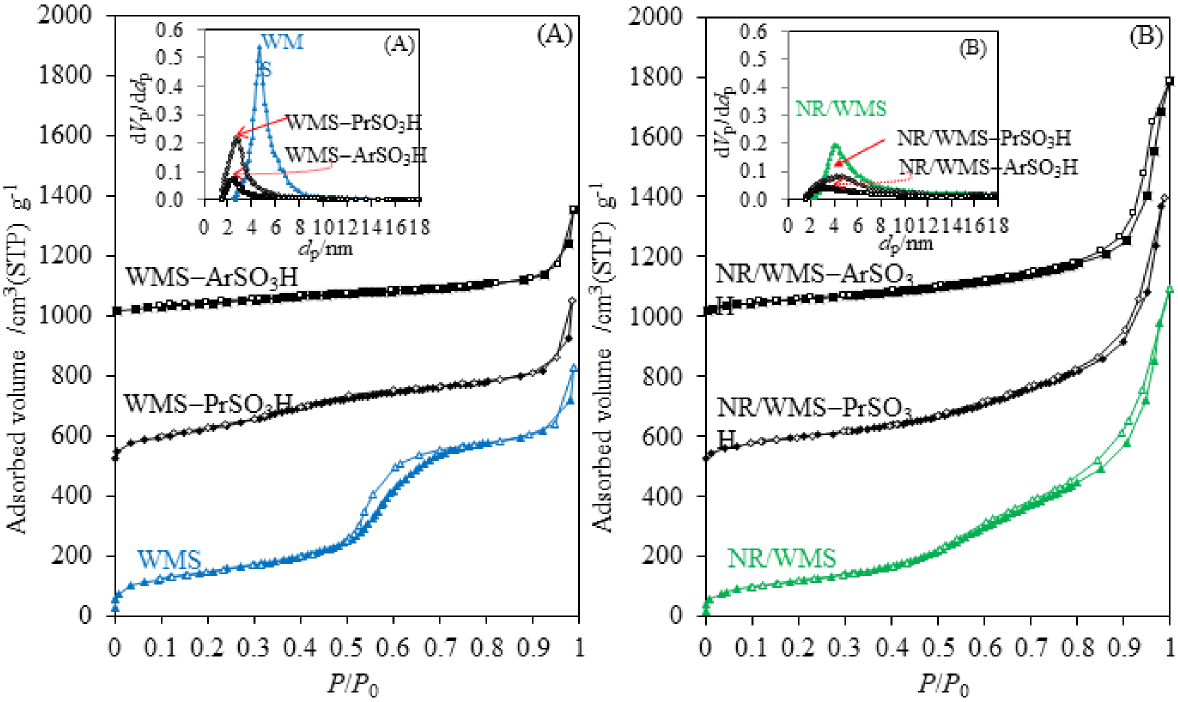

Figure 3 N_2 adsorption–desorption isotherms and BJH pore size distributions of the (A) WMS, WMS–SO_3H and (B) NR/WMS, NR/WMS–SO_3H composites.

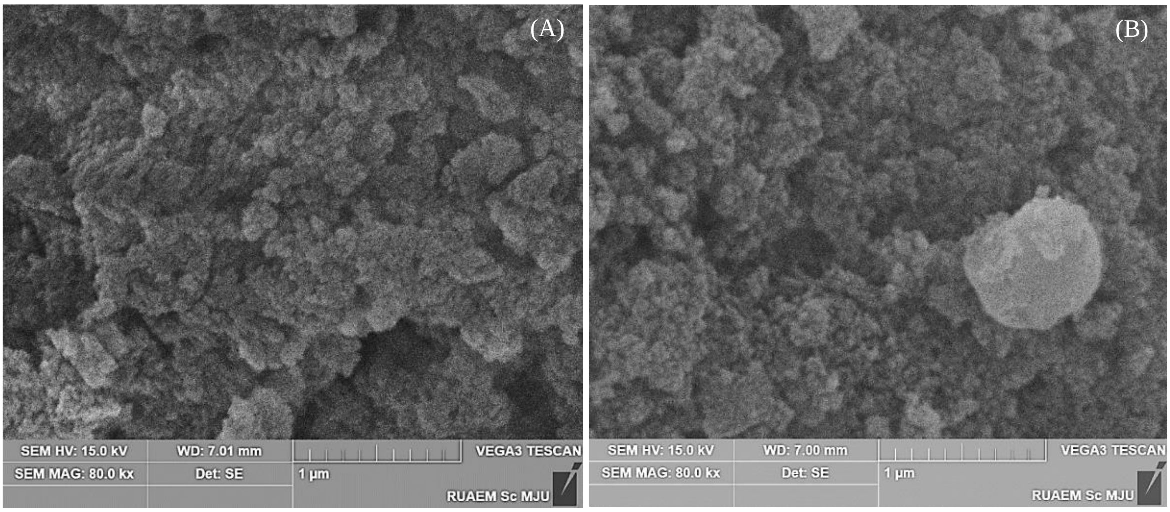

Figure 4 SEM images (80,000x magnification) of the (A) NR/WMS–$PrSO_3H$ and (B) NR/WMS –$ArSO_3H$ composites.

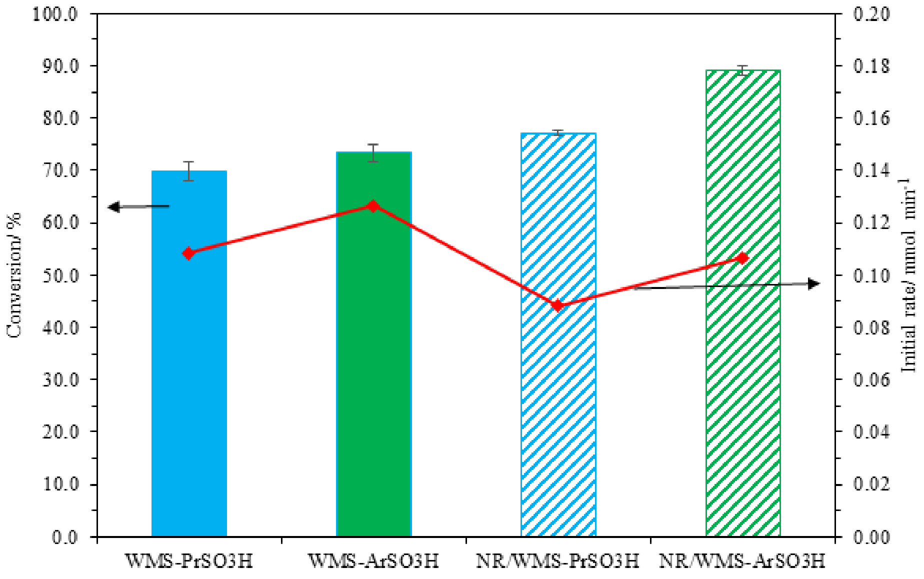

Figure 5 Esterification of palmitic acid with methanol over WMS–SO_3H materials and NR/WMS–SO_3H composites.

Conclusion

The NR/WMS functionalized with $-PrSO_3H$ and $-ArSO_3H$ groups were successfully prepared via the cocondensation method. Physical characterization techniques revealed that organosulfonic acids influenced the structural properties of the parent mesoporous silica materials, as evidenced by a decrease in the order of the mesostructure, a decrease in the BET surface area, and a change in the pore size distribution. In addition, the $-ArSO_3H$-functionalized mesoporous silica materials presented greater acidity and acid strength than did the $-PrSO_3H$ group. Moreover, NR/WMS–$ArSO_3H$, which is hydrophobic and highly acidic, resulted in the highest conversion of palmitic acid at 89.3%. Therefore, the NR/WMS–$ArSO_3H$ catalyst is a potential solid acid catalyst for biodiesel production.

Acknowledgement

The authors are grateful for the financial support from the Thailand Science Research and Innovation (TSRI), annual government statement B.E. 2567. The authors also acknowledge technical support from the Center of Excellence in Catalysis for Bioenergy and Renewable Chemicals (CBRC), and Center of Excellence on Petrochemical and Materials Technology (PETROMAT), Chulalongkorn University.

References

[1] Kuepethkaew, S., Klomklao, S., Phonsatta, N., Panya, A., Benjakul, S., Kishimura, H. Utilization of Nile tilapia viscera oil and lipase as a novel and potential feedstock and catalyst for sustainable biodiesel production. Renewable Energy, 2024, 236, 121514.

[2] Li, K., Xie, W. Enhanced biodiesel production from low-value acidic oils using ordered hierarchical macro–mesoporous MoAl@H-SiO_2 catalyst. Fuel, 2024, 364, 131105.

[3] Huang, Z., Yang, Y.C., Wang, X., Cai, R., Han, B. Biodiesel synthesis through soybean oil trancesterification using choline-based amino acid ionic liquids as catalysts. Industrial Crops & Products, 2024, 208, 117869.

[4] Zhang, Q., Zhang, C., Wu, Q., Liu, J., Song, D., Guo, Y. Sustainable production of biodiesel and transformation of glycerol to glycerol laurate esters over inner diameter-controlled sulfonic acid functionalized ethyl-bridged-organosilica nanotubes. Applied Catalysis A, General, 2021, 611, 117973.

[5] Savaliya, M.L., Tank, R.S., Dholakiya, B.Z. Rational design of hierarchically porous sulfonic acid and silica hybrids with highly active sites for efficient catalytic biodiesel synthesis. Chemistry of Inorganic Materials, 2023, 1, 100005.

[6] Wang, Y., You, J., Liu, B. Preparation of mesoporous silica supported sulfonic acid and evaluation of the catalyst in esterification reactions. Reaction Kinetics, Mechanisms and Catalysis, 2019, 128, 493–505.

[7] Testa, M.L., Parola, V.L., Venezia, A.M. Transesterification of short chain esters using sulfonic acid-functionalized hybrid silicas: Effect of silica morphology. Catalysis Today, 2014, 223, 115–121.

[8] Nuntang, S., Poompradub, S., Butnark, S., Yokoi, T., Tatsumi, T., Ngamcharussrivichai, C. Organosulfonic acid-functionalized mesoporous composites based on natural rubber and hexagonal mesoporous silica. Materials Chemistry and Physics, 2014, 147, 583–593.

[9] Nuntang, S., Yokoi, T., Tatsumi, T., Ngamcharussrivichai, C. Enhanced esterification of carboxylic acids with ethanol using propylsulfonic acid-functionalized natural rubber/ hexagonal mesoporous silica nanocomposites. Catalysis Communications, 2016, 80, 5–9.

[10] Na Lumphoon, K., Ngampradit, S., Yousatit, S., Yokoi, T., Ngamcharussrivichai, C., Nuntang, S. Tunable organosulfonic acid-functionalized natural rubber/wormhole-like mesostructured silica nanocomposites for enhancing the esterification of carboxylic acids with methanol. ScienceAsia, 2024, 50S(1), 1–11.

[11] Hamoudi, S., Royer, S., Kaliaguine, S. Propyl- and arene-sulfonic acid functionalized periodic mesoporous organosilicas. Microporous and Mesoporous Materials, 2004, 71, 17–25.

[12] Geszke-Moritz, M., Moritz, M. Modeling of boldine alkaloid adsorption onto pure and propyl-sulfonic acid-modified mesoporous silicas. A comparative study, Materials Science and Engineering: C., 2016, 69, 815–830.

[13] Pizzolitto, C., Ghedini, E., Taghavi, S., Menegazzo, F., Cruciani, G., Peurla, M., Eränen, K., Heinmaa, I., Aho, A., Kumar, N., Murzin, D.Y., Salmi, T., Signoretto, M. Acid sites modulation of siliceous-based mesoporous material by post synthesis methods. Microporous and Mesoporous Materials, 2021, 328, 111459.

[14] Vera-Baquero, F.L., Gañán, J., Morante-Zarcero, S., Sierra, I. Chiral HPLC-MS/MS determination of hyoscyamine enantiomers in baby herbal infusions after preconcentration with sulfonic HMS mesostructured silica synthesized by co-condensation. Microchemical Journal, 2024, 198, 110150.

[15] Mbaraka, I.K., Radu, D.R., Lin, V.S.Y., Shanks, B.H. Organosulfonic acid-functionalized mesoporous silicas for the esterification of fatty acid. Journal of Catalysis, 2003, 219, 329–336.

[16] Chaowamalee, S., Yan, N., Ngamcharussrivichai, C. Propylsulfonic acid-functionalized mesostructured natural rubber/silica nanocomposites as promising hydrophobic solid catalysts for alkyl levulinate synthesis. Nanomater, 2022, 12, 604.

[17] Hamoudi, S., Royer, S., Kaliaguine, S. Propyl- and arene-sulfonic acid functionalized periodic mesoporous organosilicas. Microporous and Mesoporous Materials, 2004, 71, 17–25.

[18] Rác, B., Molnár, Á., Forgo, P., Mohai, M., Bertóti, I. A comparative study of solid sulfonic acid catalysts based on various ordered mesoporous silica materials. Journal of Molecular Catalysis A: Chemical, 2006, 244, 46–57.